

PROCEEDINGS OF SPIE

[SPIDigitalLibrary.org/conference-proceedings-of-spie](https://spiedigitallibrary.org/conference-proceedings-of-spie)

Two-frequency MOPA diode laser system for difference-frequency generation of coherent THz waves

Shuji Matsuura, Pin Chen, Geoffrey A. Blake, John C. Pearson, Herbert M. Pickett

Shuji Matsuura, Pin Chen, Geoffrey A. Blake, John C. Pearson, Herbert M. Pickett, "Two-frequency MOPA diode laser system for difference-frequency generation of coherent THz waves," Proc. SPIE 3617, Terahertz Spectroscopy and Applications, (29 April 1999); doi: 10.1117/12.347126

SPIE.

Event: Optoelectronics '99 - Integrated Optoelectronic Devices, 1999, San Jose, CA, United States

Two-frequency MOPA diode laser system for difference frequency generation of coherent THz-waves

Shuji Matsuura*^a, Pin Chen^a, Geoffrey A. Blake^a, J. C. Pearson^b, Herbert M. Pickett^b

^aDiv. of Geological and Planetary Sciences, California Institute of Technology, Pasadena, CA 91125

^bJet Propulsion Laboratory, California Institute of Technology, Pasadena, CA 91109

ABSTRACT

We developed a tunable, cavity-locked diode laser source at 850 nm for difference-frequency generation of coherent THz-waves. The difference frequency is synthesized by three fiber-coupled external-cavity diode lasers, where two of the lasers are locked to adjacent modes of an ultra-stable Fabry-Perot cavity and the third laser is offset-phase-locked to the second cavity-locked laser using a tunable microwave oscillator. The first cavity-locked laser and the offset-locked laser produces the difference frequency, whose value is precisely determined by sum of integer multiple of free spectral range of the Fabry-Perot cavity and the offset frequency. The difference-frequency signal is amplified to 500 mW by the master oscillator power amplifier (MOPA) technique, simultaneous two-frequency injection-seeding with a single semiconductor optical amplifier. Here we demonstrate the difference-frequency generation of THz waves with the low-temperature-grown GaAs photomixers and its application to high-resolution spectroscopy of simple molecules. An absolute frequency calibration was carried out with an accuracy of $\sim 10^{-7}$ using CO lines in the THz region.

Keywords: terahertz, source, photomixing, diode laser, stabilization, calibration

1. INTRODUCTION

Terahertz (THz) or far-infrared frequency region lies in the gap between near-optical frequency where solid-state lasers are available and microwave frequency where electronic sources exist, and the coherent technology in this region is still in research phase. Development of the THz coherent source technology will lead to opening up a frontier in optical science.¹ THz frequencies are suitable for study of low energy light-matter interactions, such as phonon interactions in solids, rotational transitions in molecules, vibration-rotation-tunneling behavior in weakly bound clusters, and electronic fine structure in atoms. Spectroscopic observation and coherent control of these physical processes by the THz field are attractive subjects in fundamental physics, and these fundamentals are applicable to broad area in science and engineering, such as astronomy, remote sensing, and bio-medical sciences. In most of such THz applications, the frequency accuracy and tunability rather than the source power are critical to obtain meaningful results. For example, the local oscillator source for THz heterodyne receiver for astronomy require small source power ($\ll 1$ mW) but narrow line and wide tunability that it should be able to detect molecular lines from nearby interstellar clouds with the linewidth of $< 10^{-5}$ and to search for the highly redshifted lines from distant galaxies.

On the motivation described above, various type of THz sources, such as solid and molecular gas lasers, backward-wave oscillator, free-electron lasers, harmonic up-conversion from microwave sources, have been developed. Most of these sources can provide high power radiation but, until now, suffered from poor frequency tunability or pulsed oscillation. Difference-frequency generation (DFG), frequency down-conversion from optical sources, has been known as a promising technique to develop highly tunable coherent source in the THz region. Optical heterodyne mixing (photomixing) in ultra-fast photoconductor (photomixer) is an attractive down-conversion method at ~ 1 -2 THz range because of relatively high conversion efficiency compared with the DFG with nonlinear optical materials.^{2,3} Diode-laser-based systems have many advantages of compactness, low power consumption, and long lifetime.^{4,5} These properties are important to build instruments not only for satellite remote sensing and space telescope but also for laboratory spectroscopy. Although some laboratory spectroscopic studies with such THz sources have been done by several authors,⁶⁻⁸ the frequency accuracy of the THz wave has not been sufficient for high-resolution spectroscopy and heterodyne local oscillator applications.

* Correspondence: Email: matsuura@gps.caltech.edu; Telephone: 626 395 3377; Fax: 626 585 1917

In this paper we present a method for synthesizing difference frequency with the precision necessary for the advanced spectroscopic applications. A precise difference frequency is synthesized by three external-cavity diode lasers, where two of the lasers are locked to adjacent modes of an ultra-stable Fabry-Perot cavity and the third laser is offset-phase-locked to the second cavity-locked laser using a tunable microwave oscillator. The first cavity-locked laser and the offset-locked laser produces the difference frequency, whose value is precisely determined by sum of integer multiple of free spectral range of the cavity and the offset frequency. The concept of this difference-frequency synthesis is demonstrated with constructing a diode laser system at 850 nm and generating THz wave with LTG-GaAs photomixers. The difference-frequency signal (two-frequency laser output) is amplified by the master oscillator power amplifier (MOPA) technique, simultaneous two-frequency injection-seeding with a single semiconductor optical amplifier at 850 nm, to provide sufficient power to generate THz waves efficiently by photomixing in photoconductors or nonlinear materials.

2. LASER SYSTEM DESIGN AND PERFORMANCE

2.1. Master laser system

The master oscillator for the MOPA system to synthesize a precise difference frequency consists of three external-cavity diode lasers as is depicted in Fig. 1. Each laser assembly consists of an SDL5722 852 nm, 150 mW, distributed Bragg-reflector (DBR) diode laser, a collimating lens, an external cavity comprised of a 4% partial reflector mounted on a piezoelectric transducer (PZT), a 60-dB isolator, an anamorphic prism pair to circularize the laser beam, and a focusing lens to fiber couple the beam. The partial reflector and the DBR laser chip constitute an external-cavity. The laser frequency is continuously tunable within ~ 5 GHz by changing the cavity length with the PZT voltage, and coarse frequency tuning spanned ~ 700 GHz is available by changing the laser temperature. Alignment of the laser assembly is maintained by a compact aluminum rail structure. All the optical components to control and stabilize laser frequencies are implemented in polarization-maintaining (PM) single-mode fiber as is shown in Fig. 1. The fiber optics offer flexibility, compactness, insensitivity to vibration, ease of optical alignment, and eye protection. The optical fiber also serves as a spatial filter, allowing two different laser frequencies to be combined with nearly perfect spatial mode overlap. The latter is critical in the Fabry-Perot cavity alignment, in achieving equal amplification in the final MOPA amplifier, and in efficient photomixer operation. The fiber output of the #1 and #3 lasers, depicted as P1 and P3, are combined together with a 3-dB directional coupler and used for the photomixing. Unfortunately, the total maximum power of the dual-frequency output from the final 3-dB fiber coupler was limited to approximately 30 mW mainly due to insertion loss of optical radiation to the fiber and coupling loss at the fiber connectors.

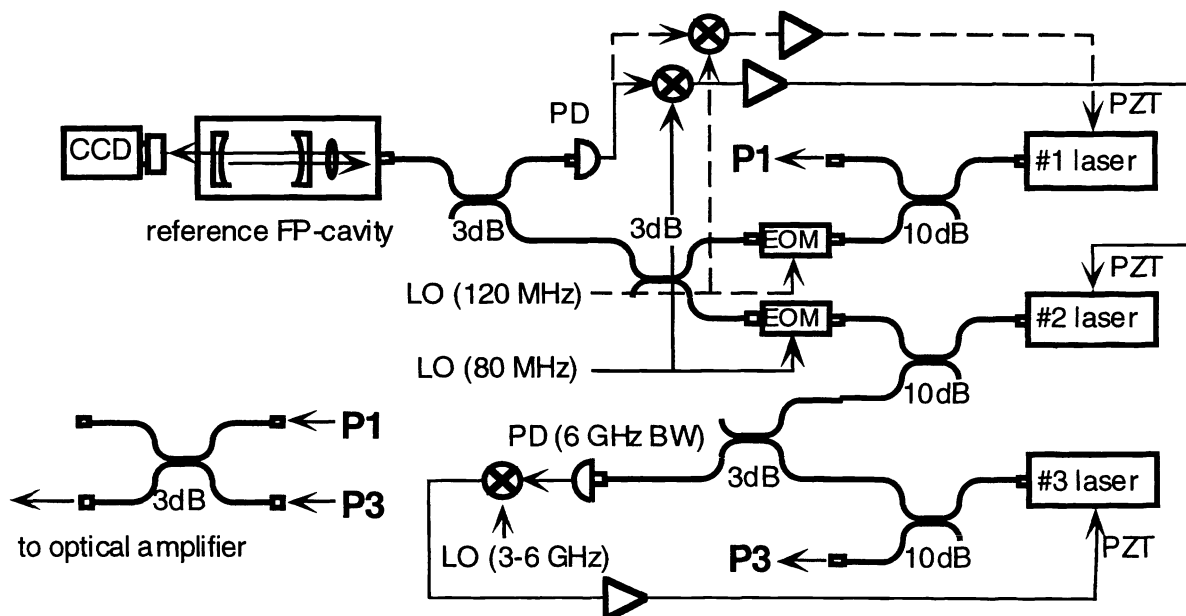


Fig. 1: Schematic diagram of the master laser system that synthesize a precise difference frequency.

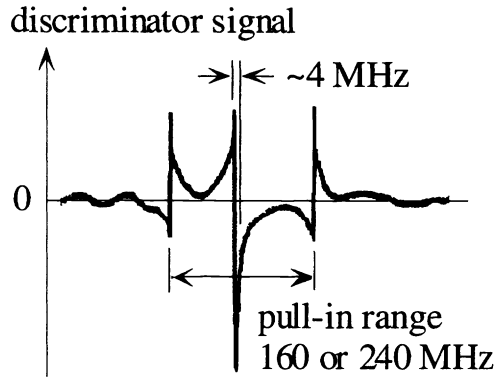


Fig. 2: The dispersion signal of the cavity fringe used for the frequency stabilization.

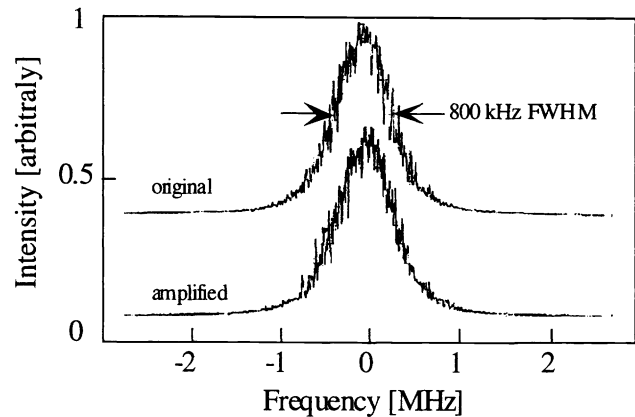


Fig. 3: The spectrum of the beat note signal between the #1 and #3 lasers before (upper) and after (lower) amplification.

The #1 and #2 lasers are cross-polarized and locked to different longitudinal modes of an ultra-low-expansion (ULE) Fabry-Perot (FP) cavity by the Pound-Drever-Hall (PDH) method.^{9,10} The ULE cavity material has a thermal expansion coefficient at room temperature of $\alpha = -2 \times 10^{-10} \text{ }^\circ\text{C}^{-1}$, which is comparable to the stability of a quartz reference oscillator in conventional microwave sources. For the PDH method FM sidebands are generated on the two cavity-locked lasers with electro-optic phase modulators (EOM) operating at 80 MHz and 120 MHz. To verify coupling to the fundamental longitudinal cavity mode, the transmitted beam profile was monitored by a CCD-camera. The difference frequency between the two cavity-locked lasers is discretely tunable in steps of the cavity free spectral range (FSR). The phase of the beam reflected from the cavity is compared to the modulation frequency in a frequency multiplier. When the laser frequency is within the modulation frequency of the cavity resonance, the output of the frequency multiplier provides a DC frequency dispersion which crosses zero at the cavity resonance. Fig. 2 shows the dispersion curve at the mixer output obtained by sweeping the laser frequency through the cavity resonance. The central linear portion of the dispersion curve centered at the cavity is used to generate an error signal voltage, which is fed back to the PZT of the external laser cavity with a simple servo electronic circuit consisting of an integrator and an amplifier. The linear part of frequency discriminator shown in Fig. 2 is ~ 4 MHz, in accordance with the FSR of the cavity of 3 GHz and its finesse of 750. In the present laser system, the loop bandwidth of the PZT control circuit was limited to 3 kHz to avoid acoustic resonances in the support structure of the partial reflector with the PZT.

The third laser (#3) is locked to a beat note signal between the #2 and #3 lasers detected by a 6 GHz bandwidth photodetector and compared to tunable frequency generated by a microwave synthesizer. In order to implement a phase-lock with the same electronics as the cavity-lock, the signal was split with one arm sent through a delay line, and the resulting phase shift between the two signals was used to generate the error signal for the PZT of the #3 laser. The offset frequency is measured precisely by a microwave counter locked to a high precision reference, making any drifts or offsets in the phase lock scheme irrelevant to the system calibration. The offset frequency can be continuously tuned over 5 GHz by stepping the synthesizer frequency and tracking the PZT voltage. The maximum sweep rate of ~ 100 MHz/s is limited by the feedback loop bandwidth. The difference frequency between the #1 and #3 is determined by the sum of integral multiples of the FSR (3 GHz) of the reference cavity and the microwave offset frequency. The accuracy of the difference frequency is determined by the accuracy of the FSR measurement along with any DC offset in the electrical portions of the lock loops. The microwave offset frequency is locked to a high accuracy ($\sim 10^{-12}$) reference source and measured by a counter locked to the same reference in order to correct in real time any electrical offset in that lock loop.

In the laboratory environment there are relatively large temperature changes and the resulting changes of temperature equilibrium in the external cavity and laser themselves. The PZT voltage generally compensates for these drifts, but they were occasionally large enough to exceed the PZT error signal limit. The drift could be dramatically reduced by putting the laser rails on a temperature-controlled base plate. Once this was done, all-day-long cavity-locks of the laser have been routinely achieved without adjusting the temperature of the laser itself.

The overall system performance was assessed by observing a beat note between the #1 and #3 lasers with a 25 GHz bandwidth photodetector and a spectrum analyzer. The upper curve in Fig. 3 represents a 12 GHz beat spectrum for a 1-s integration time and a spectral resolution of 100 kHz. The FWHM spectral power bandwidth is approximately 800 kHz. The short-term linewidth of each laser is determined entirely by the optical feedback from the external cavity because the 3 kHz bandwidth of the lock loop circuit is much less than the laser linewidth.

2.2. Two-frequency MOPA operation

The two-frequency output of the master laser system was injection-seeded to an optical amplifier.¹¹ The two-frequency MOPA operation has the advantages of high power output and guarantees excellent spatial overlap of the two frequency beams, which is essential for efficient optical-heterodyne conversion.

The amplifier part of the MOPA system is shown in Fig. 4. A single traveling-wave 850 nm semiconductor tapered optical amplifier, which was the central component of a commercial external-cavity single-mode laser (SDL8630), was used. The fiber output from the master laser system was collimated, passed through a 60-dB optical isolator, and sent to a half-wave plate for fine adjustment of the polarization. The circular beam was transformed into an elliptical shape by an anamorphic prism pair in order to match its spatial mode to the amplifier $1 \times 3 \mu\text{m}$ input facet. The master laser beam is injected into the optical amplifier chip. The amplified output beam is spatially filtered and collimated to a 3 mm diameter Gaussian beam by a telescope.

The amplifier was operated under highly saturated conditions at an injection laser power of 10 mW. The output power was relatively insensitive to both the injection power and frequencies and constant within 5% over the entire range of the difference frequency (<1.3 THz). The amplifier used in the present system was a component of a commercial external-cavity single-mode laser, and one of the amplifier chip facets was anti-reflection coated but the other facet was not. Small variations in the output power with a period of ~ 15 GHz caused by the amplifier chip mode were observed.

Another desirable MOPA property for photomixing is that the gain for the two injected frequencies is nearly equal to each other. As expected, the output power ratio between the two frequency components was close to unity over a wide range of difference frequencies, specifically from ~ 10 GHz -- 1.3 THz. The small variations caused by the chip mode structure in the power ratio were also observed. Unbalanced amplification between the two frequencies occurred only at difference frequencies lower than 10 GHz. This behavior can be interpreted as arising from the interaction of the two frequency components driven by the refractive index change induced by the carrier density modulation at the difference frequency.¹¹ Therefore, the lower frequency limit of the well-balanced two-frequency amplification is determined by the carrier lifetime of the amplifier. As shown in Fig. 3, the spectrum of beat signal between the amplified two frequency components was identical to that of the master laser as long as the difference frequency was greater than 10 GHz.

3. SPECTROSCOPY APPLICATIONS

As described above, the two-frequency laser system allows DFG of THz-waves in ultra-fast photoconductors or other nonlinear optical media. Here, we demonstrate the performance of the laser system with high resolution rotational spectroscopy of the simple molecules acetonitrile (CH_3CN) and carbon monoxide (CO). Due to the lack of spectral analysis techniques in the THz region, spectroscopic measurements provide one of the best diagnosis of frequency and spectral purity.

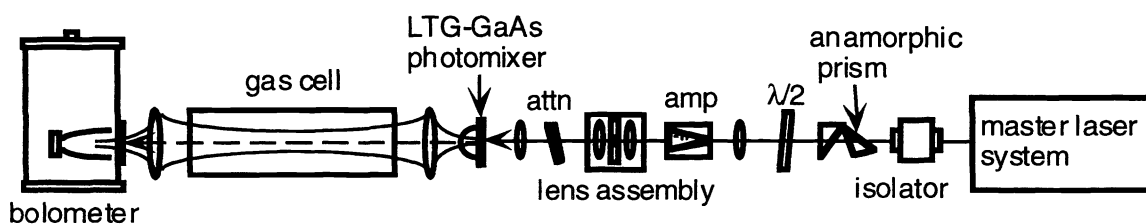


Fig. 4: Schematic diagram of the optical amplifier and spectroscopy setup.

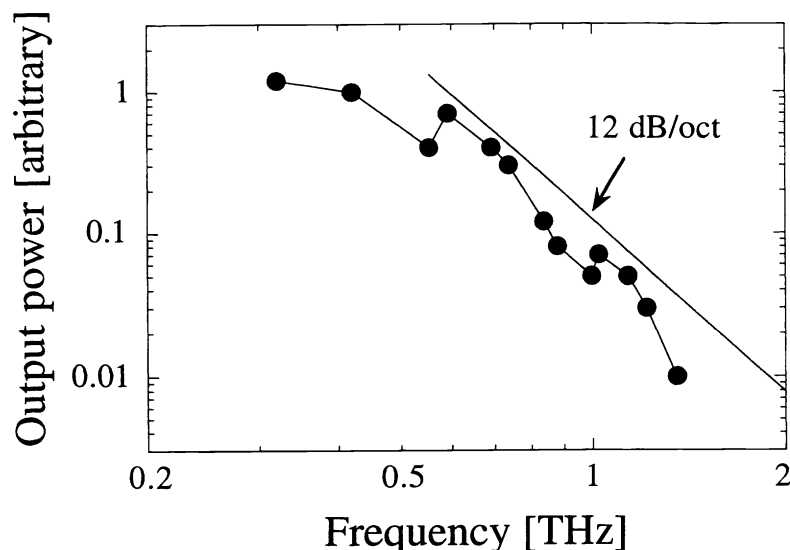


Fig. 5: The frequency dependence of the output power generated by the THz photomixer. The solid line represents the theoretical roll-off behavior with the slope of 12 dB/oct.

3.1. THz-wave generation

The LTG-GaAs photomixer used in the present experiment was grown on a semi-insulating GaAs substrate, and a planar log-spiral antenna with 0.2- μm interdigitated electrodes and 1.8- μm gaps in a $8 \times 8 \mu\text{m}$ active area was etched on the wafer.¹² The photomixer was mounted on the flat surface of a hyper-hemispherical lens made of high-resistivity silicon. Most of the generated radiation is emitted into free space through the photomixer substrate and the silicon lens. A DC bias voltage of 20 V was applied to the electrodes by a constant current supply set at 0.5 mA for a pump laser power of 30 mW. Under these conditions, the photomixer provided a maximum output power of $\sim 0.1 \mu\text{W}$ at 1 THz, while the 3 dB bandwidth of the generated THz-waves was approximately 700 GHz, as is shown in Fig. 5. The spectral bandwidth and the frequency roll-off behavior is roughly consistent with the carrier lifetime of the LTG-GaAs of $t \sim 200\text{-}300$ fs and the photomixer RC time constant, where $R = 72 \Omega$ is the radiation impedance and $C = 0.5$ fF is the electrode capacitance.¹² The output power can be improved by increase of the pump laser power, but the laser power was kept well below the safe level (< 50 mW) to prevent the photomixer from thermal damage.

3.2. Spectroscopy

The experimental setup used for spectroscopy is shown Fig. 4. The two-frequency output from the MOPA was appropriately attenuated (~ 30 mW) and focused onto the photomixer. The THz output beam was collimated with a combination of the silicon hyper-hemispherical lens and a Teflon lens and passed through an 8 cm long 1 inch diameter gas cell fitted with polyethylene windows. The beam transmitted through the cell was weakly focused with a Teflon lens and fed into a 4.2 K InSb hot-electron bolometer or a 1.6 K composite Si bolometer. The tone-burst modulation method was used to obtain absorption spectra of molecules.¹³ The advantage of the tone-burst method for THz spectroscopy as compared to traditional FM modulation is that sensitive detection with slow detectors such as silicon composite bolometers can be achieved. The injection current of the #1 cavity-locked laser was modulated with a 2 MHz tone, above the cavity-lock loop bandwidth, at a 10 kHz burst rate. A lock-in amplifier, detecting at 10 kHz, was used to demodulate the detector signal generating the traditional second derivative of molecular absorption features.

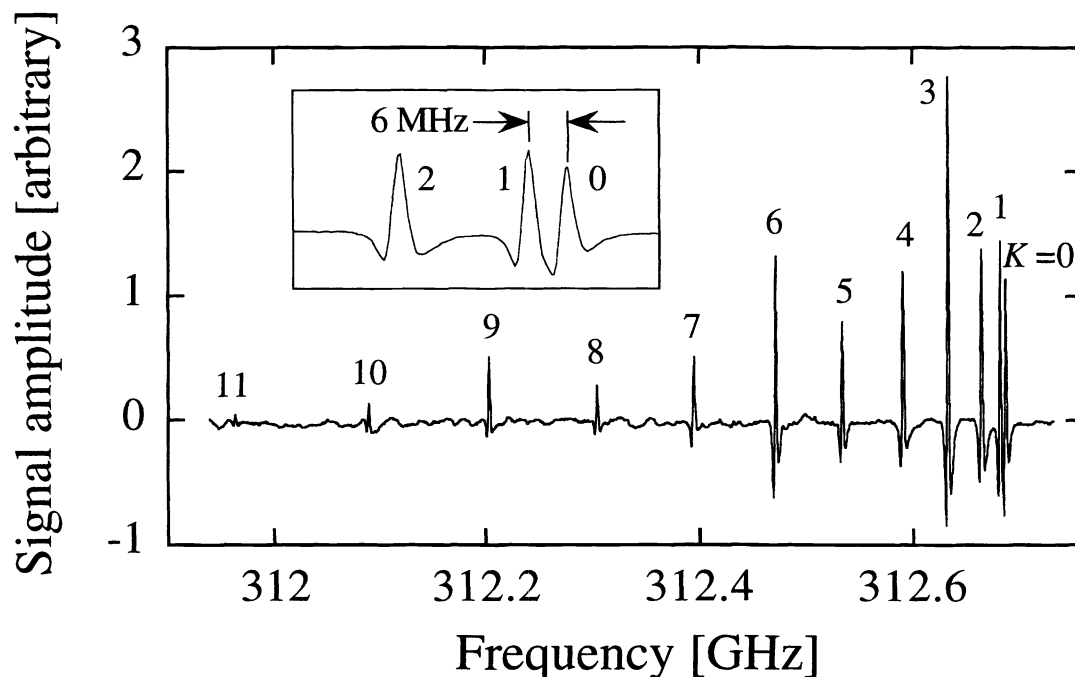


Fig. 6: The second-derivative absorption spectrum of $\text{CH}_3\text{CN } J = 16 \rightarrow 17$ rotational transitions near 312 GHz. The spectrum for ordinary $^{12}\text{CH}_3^{12}\text{CN}$. The inset is expanded view of the $K = 0-2$ lines.

Fig. 6 presents the absorption spectrum of the $\text{CH}_3\text{CN } J_K = 16_K \rightarrow 17_K$ rotational transitions near 312 GHz. The spectrum was taken with a sweep rate of 2 MHz/sec, and is plotted as a function of the microwave offset frequency. The data was recorded at 7 sample/sec with a lock-in amplifier. The spectrum shows the well known K-structure of a symmetric-top, with K components from $K = 0-11$ assigned in the spectrum. As seen in the inset of Fig. 8(a), the $K = 0, 1$ lines, which are separated by ~ 6 MHz, are clearly resolved. The gas pressure was 60 mTorr, and the observed line widths are consistent with a convolution of pressure broadened linewidths and the instrument response. The minimum detectable absorption of this system is estimated to be $\sim 10^{-5}$, and is detector-noise-limited. The result indicates that the spectral purity, frequency control, and the output power of this system is sufficient for the laboratory spectroscopic study of molecules at THz frequencies.

3.2. Frequency calibration

For further spectroscopic measurements such as the search for unknown molecular lines and for use in astronomical observations, absolute frequency calibration of the difference frequency is necessary. Since the accuracy of the difference frequency is defined by the reference FP-cavity, the calibration must include a precise measurement of the FSR of the cavity. In principle, the difference frequency can be determined to within $\sim 10^{-10} \text{ }^\circ\text{C}^{-1}$, the temperature-fluctuation-limited accuracy, according to the thermal expansion coefficient of the ULE material. Well known molecular lines in the THz region, such as the rotational transitions of carbon monoxide (CO), are suitable for accurate calibration, since the frequencies of these THz molecular transitions correspond to ~ 300 times the FSR and can be easily measured to within an accuracy of 10^{-7} . A number of measurements and the careful use of statistics should allow the accuracy of 10^{-8} .

Pure rotational transitions of CO were measured using the same configuration as the acetonitrile measurements, except that a composite silicon bolometer was used in these measurements. According to the conventional model for the diatomic

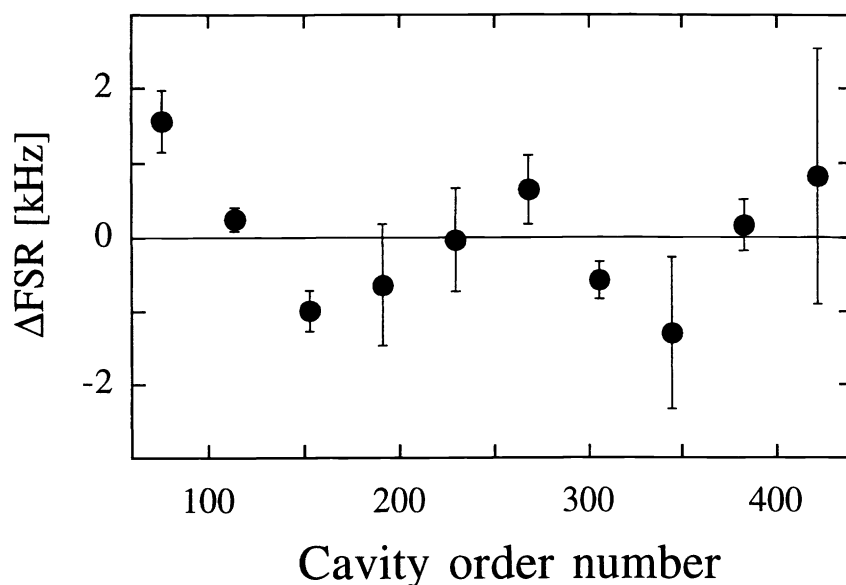


Fig. 7: The result of the FSR measurements by CO lines for $J = 1-10$. The deviation of the FSR values from their average are shown as a function of the cavity order difference.

$^{12}\text{C}^{16}\text{O}$ molecule, the rotational transition lines should appear at frequencies of $\nu = (W_{J+1} - W_J) / h$, and $W_J / h = BJ(J+1) - DJ^2(J+1)^2 + HJ^3(J+1)^3$, where $B = 57,635.9660$ MHz, $D = 0.1835053$ MHz, $H = 1.731 \times 10^{-7}$ MHz, h is Planck constant, and J is an integer.¹⁴ Absorption measurements for CO lines with $J = 1-10$ over the range of 230 GHz to 1267 GHz were carried out by measuring the microwave offset frequency, ν_{offset} , and counting the number of cavity orders between the two cavity-locked lasers. The line position was determined by fitting a parabola to the center of the 2nd derivative line profile. The cavity FSR for each CO line is simply calculated by dividing $\nu - \nu_{offset}$ by the cavity order difference, because the DC offset of the difference frequency caused by the DC offset voltage of the lock loop circuit was statistically insignificant. From this data set, the average of the FSR value for all CO line measurements was determined to be $2,996,757.48 \pm 0.10$ kHz. Fig. 7 shows the deviation of the FSR values from their average as a function of the cavity order difference. Even if the scatter of the data around the average value is a real frequency dispersion of the cavity, the frequency dependence of the FSR over a 1.3 THz span is constant to within 1 kHz. In this approach, the frequency accuracy is limited by our ability to determine the center of the line profiles, which in turn depends on the instrumental resolution and the signal-to-noise ratio of the spectrum. The calibration accuracy can therefore be improved by increasing the source power and/or improving the detector sensitivity.

4. FUTURE DIRECTION

The photomixer used in the experiments reported here provides a maximum output power of approximately $0.1 \mu\text{W}$ at 1 THz for a pump laser power of 30 mW. A straightforward extrapolation of the quadratic dependence of the THz-wave power on the laser power leads to the prediction that some $10 \mu\text{W}$ of power should be obtainable using the present laser system, whose maximum 850 nm power is 500 mW. However, the maximum pump laser power is currently limited to approximately 50 mW by thermal damage threshold of the photomixer.¹⁴ To solve this thermal problem, photomixers with distributed electrode structures and higher thermal conductivity substrates are being developed.^{12,15} We have recently designed and operated an optical/THz velocity-matched traveling-wave photomixer that can handle 1-W level pump laser power. These photomixers can be driven at the full output of the high-power laser system reported here, and will ultimately produce power levels over $1 \mu\text{W}$ at 1 THz.

The three laser difference-frequency generation and control method presented here is quite general and could be extended to a large number of different lasers. The absolute calibration method is also quite general and can be widely employed. This

frequency control technique is especially important in the >1-2 THz region, where comparison to a harmonically up-converted frequency reference may be difficult or impossible. The use of a MOPA as a two-frequency amplifier should facilitate the use of this control method with the next generation of photomixers based on nonlinear optical media such as LiNO₃, GaP, GaAs, and quantum-well materials. At optical source frequencies DFG using nonlinear optical materials might be more efficient than electro-optical down-conversion with photoconductors, because the efficiency of the nonlinear optical DFG has a ν^4 dependence in the long wavelength limit.¹⁶ Further development of nonlinear optical materials and novel devices with large χ^2 at diode laser frequencies are expected in the near future, making precision difference frequency generation essential for their use as THz sources.

ACKNOWLEDGMENT

The authors thank S. Verghese and K. A. McIntosh of MIT Lincoln Laboratory for preparing the LTG-GaAs photomixers. We also thank T. J. Crawford of Jet Propulsion Laboratory for his technical support. Portions of this work performed at the Jet Propulsion Laboratory California Institute of Technology were done under contract with the National Aeronautics and Space Administration (NASA). G. A. Blake acknowledges additional support from NASA and from the National Science Foundation.

REFERENCES

1. R. Datla, E. Grossman, and M.K. Hobish, eds. *Metrology Issues in Terahertz Physics and Technology*, NIST vol. 5701, 103 pp., 1995.
2. E.R. Brown, F.W. Smith, and K.A. McIntosh, "Coherent Millimeter-Wave Generation by Heterodyne Conversion in Low-Temperature-Grown GaAs Photoconductors," *J. Appl. Phys.*, vol. 73, pp. 1480-1484, 1993.
3. E.R. Brown, K.A. McIntosh, K.B. Nichols, and C.L. Dennis, "Photomixing up to 3.8 THz in Low-Temperature-Grown GaAs," *Appl. Phys. Lett.*, vol. 66, pp. 285-287, 1995.
4. K.A. McIntosh, E.R. Brown, K.B. Nichols, O.B. McMahon, W.F. DiNatale, and T.M. Lyszczarz, "Terahertz Photomixing With Diode-Lasers in Low-Temperature-Grown GaAs," *Appl. Phys. Lett.*, vol. 67, pp. 3844-3846, 1995.
5. S. Matsuura, M. Tani, and K. Sakai, "Generation of Coherent Terahertz Radiation by Photomixing in Dipole Photoconductive Antennas," *Appl. Phys. Lett.*, vol. 70, pp. 559-561, 1997.
6. A.S. Pine, R.D. Suenram, E.R. Brown, and K.A. McIntosh, "A Terahertz Photomixing Spectrometer -- Application to SO₂ Self-Broadening," *J. Mol. Spec.*, vol. 175, pp. 37-47, 1996.
7. P. Chen, G.A. Blake, M.C. Gaidis, E.R. Brown, K.A. McIntosh, S.Y. Chou, M.I. Nathan, and F. Williamson, "Spectroscopic Applications and Frequency Locking of THz Photomixing with Distributed-Bragg-Reflector Diode Lasers in Low-Temperature-Grown GaAs," *Appl. Phys. Lett.*, vol. 71, pp. 1601-1603, 1997.
8. S. Matsuura, M. Tani, H. Abe, K. Sakai, H. Ozeki, and S. Saito, "High Resolution THz Spectroscopy by a Compact Radiation Source Based on Photomixing with Diode Lasers in a Photoconductive Antenna," *J. Mol. Spec.*, vol. 187, pp. 97-101, 1998.
9. R.V. Pound, *Rev. Sci. Instrum.*, vol. 17, pp. 490-505, 1946.
10. R.W.P. Drever, J.L. Hall, F.V. Kowalski, J. Hough, G.M. Ford, A.J. Munley, and H. Ward, "Laser Phase and Frequency Stabilization using an Optical Resonator," *Appl. Phys. B*, vol. 31, pp. 97-105, 1983.
11. S. Matsuura, P. Chen, G.A. Blake, J.C. Pearson, and H.M. Pickett, "Simultaneous Amplification of Terahertz Difference Frequencies by an Injection-Seeded Semiconductor Laser Amplifier at 850 nm," *Int. J. of Infrared and Millimeter Waves*, vol. 19, pp. 849-858, 1998.
12. S. Verghese, K.A. McIntosh, and E.R. Brown, "Highly Tunable Fiber-Coupled Photomixers with Coherent Terahertz Output Power," *IEEE Trans. Microwave Theory and Tech.*, vol. 45, pp. 1301-1309, 1997.
13. H.M. Pickett, "Determination of Collisional Linewidths and Shifts by a Convolution Method," *Appl. Optics*, vol. 19, pp. 2745-2749, 1980.
14. I. Nolt, J.V. Radostitz, G. Dilonardo, K.M. Evenson, D.A. Jennings, K.R. Leopold, L.R. Zink, and A. Hinz, "Accurate Rotational Constants of CO, HCl, and HF -- Spectral Standards for the 0.3 to 6 THz (10 cm⁻¹ to 200 cm⁻¹) Region," *J. Mol. Spec.*, vol. 125, pp. 274-287, 1987.
15. L.Y. Lin, M.C. Wu, T. Itoh, T.A. Vang, R.E. Muller, D.L. Sivco, and A.Y. Cho, "Velocity-Matched Distributed Photodetectors with High Saturation Power and Large Bandwidth," *IEEE Photon. Technol. Lett.*, vol. 8, pp. 1376-1378, 1996.
16. Y.R. Shen, *Principles of Nonlinear Optics*. New York: John Wiley and Sons, 1984.